Earth Moon Planets (2016) 117:23–39
DOI 10.1007/s11038-016-9481-6

Transport and Distribution of Hydroxyl Radicals and Oxygen Atoms from H_2O Photodissociation in the Inner Coma of Comet 67P/Churyumov–Gerasimenko

Ian-Lin Lai[1] · Cheng-Chin Su[2] · Wing-Huen Ip[1,3,4] · Chen-En Wei[3] · Jong-Shinn Wu[2] · Ming-Chung Lo[2] · Ying Liao[5] · Nicolas Thomas[5]

Received: 15 June 2015 / Accepted: 19 January 2016 / Published online: 28 January 2016

Abstract With a combination of the Direct Simulation Monte Carlo (DSMC) calculation and test particle computation, the ballistic transport process of the hydroxyl radicals and oxygen atoms produced by photodissociation of water molecules in the coma of comet 67P/Churyumov–Gerasimenko is modelled. We discuss the key elements and essential features of such simulations which results can be compared with the remote-sensing and in situ measurements of cometary gas coma from the Rosetta mission at different orbital phases of this comet.

Keywords Comets · Comet 67P · Atmosphere · Photodissociation

1 Introduction

The main composition of cometary ice is H_2O, CO_2, CO accompanied by a myriad of minor species like CH_3OH, CH_4, NH_3 and H_2S (Biver et al. 1997; Bockelee-Morvan et al. 2004). After release from the nucleus surface the neutral gas will expand forming an extended coma. In this process, the parent molecules will be subject to photodissociation and photoionization leading to the production of daughter molecules like OH radical and oxygen atoms. In fact, the optical coma of a comet is composed mainly of dust and daughter molecules such as C_2, C_3, CN, NH and NH_2 (Feldman et al. 2004). The spatial distributions of the parent and daughter species are generally approximated by the

✉ Ian-Lin Lai
ianlai@g.ncu.edu.tw

[1] Institute of Space Sciences, National Central University, Taoyuan City, Taiwan

[2] Department of Mechanical Engineering, National Chiao Tung University, Hsinchu City, Taiwan

[3] Institute of Astronomy, National Central University, Taoyuan City, Taiwan

[4] Space Science Institute, Macau University of Science and Technology, Taipa, Macau

[5] Physikalisches Institut, University of Bern, Bern, Switzerland

spherically symmetric Haser model assuming a constant radial speed for different species (Haser 1957). The actual situation is more complicated because the outward expansion of the neutral gas has to go through the collisional zone near the nucleus until the collisionless region at large distance. In addition, the three-dimensional structure of the nucleus and anisotropic outgassing effect could limit the validity of the spherically symmetric models. It is for these reasons, numerical approaches such as the Direct Simulation Monte Carlo (DSMC) method has been applied to the cometary gas dynamics to trace the gradual development (Crifo et al. 2004; Combi et al. 2004; Zakharov et al. 2009; Tenishev et al. 2011; Rubin et al. 2011; Finklenburg et al. 2014; Liao et al. 2016).

Because of photolytic effects, the cometary parent molecules will be dissociated or ionized by solar radiation. Festou (1981) was the first to investigate the separate flow dynamics of the parent molecules and the photo-fragments. This vectorial model takes into account the original flow velocity and the additional velocity components because of the partition of the excess energy among the photo-fragments. For example, in the case of the photodissociation of the water molecules, the channel of $H_2O + h\nu \rightarrow OH + H + \Delta\varepsilon$ (branching ratio = 91.86 %) is characterized by $\Delta\varepsilon = 3.4$ eV; the other channel of $H_2O + h\nu \rightarrow H_2 + O(^1D) + \Delta\varepsilon$ (branching ratio = 4.88 %) has $\Delta\varepsilon = 3.5$ eV (Schmidt et al. 1988; Xie and Mumma 1996a). In the collisional region, the suprathermal photo-fragments are responsible for heating and acceleration of the expanding gas; the photo-fragments will escape efficiently if created in the collision-free zone (Ip 1983, 1985).

Xie and Mumma (1996a, b) investigated by means of test particle calculations the evolution of the velocity distributions of the H_2O, OH, H_2, O and H atoms in the coma of comet Halley at the time of the Giotto encounter. Combi (1996) pioneered the DSMC model calculation with the photochemistry of H_2O and CO by tracking the dynamics of six species (i.e., H_2O, CO, OH, H_2, O and H). Two cases with different gas production rates (Q), namely, one with $Q = 3 \times 10^{28}$ molecules s^{-1} and another with $Q = 6 \times 10^{29}$ molecules s^{-1}, were studied. The surface sublimation rate was characterized by strong day-night asymmetry. A fraction ($\sim$15 %) of the gas flow can reach the night side hemisphere because of the pressure gradient built up across the terminator in the collisional zone. Such a backflow effect could mean that recondensation of water ice might be possible on the night side of a slow-rotating comet nucleus. Rubin et al. (2011) investigated the coma dynamics with a multi-fluid treatment by assuming single velocity profile for many more species and their photo-fragments. Combi (1996) and Rubin et al. (2011) have their focus on the axially symmetric coma outflows. In the present work, we will explore how the DSMC method can be used to simulate the density distributions and velocity fields of the photodissociation products as a consequence of the kinetic effect in the near-coma of comet 67P/Churyumov–Gerasimenko which has a rather irregular shape.

The radius of the coma collision zone can be estimated by equating the collisional mean-free-path (λ) to the radial distance (r_c). Since $\lambda \sim (n\bar{\sigma})^{-1}$ where n is the number density of the gas molecules and $\bar{\sigma}$ ($\sim 3 \times 10^{-15}$ cm^2) is the collisional cross section, we have $r_c = \bar{\sigma}Q/4\pi v$ where Q is the gas production rate and v is the gas flow speed under the assumption of spherical symmetry. For $\bar{\sigma} \sim 3 \times 10^{-15}$ cm^2, we have $r_c = 250$ ($Q/10^{28}$ molecules s^{-1}) (10^5 cm s^{-1}/v) km. In the early phase of the Rosetta mission right after rendezvous in August–September 2014 when the comet 67P was at a heliocentric distance of 3.0–3.5 AU, Q $\sim$ 10^{25}–10^{26} molecules s^{-1} (Snodgrass et al. 2013; Gulkis et al. 2015). The coma is therefore expected to be in collisionless condition for cometocentric distances larger than a few km. There is also strong indication that the gas outflow is significantly affected by the topography and corresponding sunlit condition of the two-lobed nucleus because the outgassing activity peaked near the neck (e.g., the Hapi) region

(Sierks et al. 2015; Gulkis et al. 2015; Haessig et al. 2015; Lin et al. 2015). Comet 67P thus provides a fertile ground for new approaches in its gas flow dynamics.

Without in situ measurements or close-up observations by spacecraft, the dynamics and production rates of the water molecules emitted from cometary nucleus surfaces can be investigated by ground-based methods in radio wavelength in terms of the OH 18-cm emission (Crovisier 1989; Bockelee-Morvan et al. 1990; Tseng et al. 2007). The OH fluorescence at 3085 Å has often been used to derive the H_2O production rates in comets (Schleicher and A'Hearn 1988; Feldman et al. 2004). The forbidden oxygen line of [OI] at 6300 Å with a lifetime of about 130 s after production is also a favorite emission for the measurement of the water production rate (see Festou 1981; Fink and Johnson 1984; Cochran and Cochran 2001; Cochran 2008; Bhardwaj and Raghuran 1996).

Note that the photodissociation of the water molecules is not the only process leading to the production of [OI] 6300 Å emission. Bhardwaj and Raghuran (1996) considered the atomic oxygen green (5577 Å) and red-doublet (6300, 6364 Å) emissions in comet C/1996 B2 Hyakutake and found that CO_2 (relative abundance of 1–5 %) and CO (relative abundance of 22 %) should contribute to no more than 10 % of the red line emission. Because the relative abundance of CO_2 and CO of comet 67P are of the order of 2.7 and 2.5 %, respectively, for gas flow from the Hapi region according to the ROSINA measurements (Le Roy et al. 2015), the contribution to the photo-production of O(^{1}D) from these two volatile species is therefore small ($\sim$10 %), according to the most recent work of Raghuram et al. (2016).

It is noted that the ALICE UV spectrometer on Rosetta detected strong HI and OI emissions in the near vicinity of the comet nucleus which can only be accounted for by the photoelectron impact dissociation of H_2O and CO_2 (Feldman et al. 2015). In addition, similar electron impact effect on the O_2 molecules which have been found to be surprisingly abundant with an average mixing ratio of 3. 8 % (Bieler et al. 2005) could also be important in the production of OI (and O(^{1}D)). This means, besides direct mass spectrometer measurements (Haessig et al. 2015) and microwave spectrometer measurements of the water molecule emission at 557 GHz (Gulkis et al. 2015), the gas production rate and photoelectron impact rate of comet 67P can be estimated via ultraviolet and optical imaging observations of the OH and [OI] emission by the OSIRIS scientific camera and the ALICE UV spectrometer, respectively (Bodewits et al. 2016).

The structure of the paper is as follows. Section 2 provides a brief description and heritage of the DSMC code employed in the study. Section 3 presents the numerical results that are to be followed by a summary in Sect. 4.

2 The Model

The local Knudsen number (Kn) is used to indicate the degree of rarefaction of gas flow.

$$K_n = \frac{\lambda}{L}$$

where λ is the local mean free path. L is the characteristic length. The mean free path λ of molecule is

$$\lambda = \frac{1}{\sqrt{2}\pi\sigma^2 n}$$

where n is the number density and σ is the effective diameter of the molecule (Bird 1994). If $Kn < 0.01$, we call the gas a continuum flow. When $Kn > 0.01$, the continuum

assumption breaks down and continuum solutions fail. In the transition region between collisional and collisionless condition, Kn $\sim$ 1. And if Kn $>$ 10, it would be a free molecular flow.

As shown in Fig. 1, four regimes of the expanding cometary outflow can be defined in terms of Knudsen number.

1. Kn $\rightarrow$ 0: The flow is a continuum flow which can satisfy the Euler equations and neglect molecular diffusion.
2. Kn $< 10^{-3}$: The flow is a continuum flow and it is accurately modeled by the Navier–Stokes equations with no-slip boundary conditions
3. $10^{-3} <$ Kn $< 10^{-1}$: The flow still can satisfy the Navier–Stokes equations with a slip boundary condition.
4. $10^{-1} <$ Kn < 10: The flow is in a transition regime and the continuum approach of the Navier–Stokes equations is no longer valid. However, the intermolecular collisions are not yet negligible and should be taken into account.
5. Kn > 10: The flow is in a free molecular region and the occurrence of intermolecular collisions can be neglected.

Figure 2 illustrates the dimension of the collisional zone around comet 67P at different heliocentric distances. It can be seen that, when the heliocentric distance of 67P is larger than 1.5 AU, collisional process and the transition to collision-free flow condition must be taken into consideration in determining the density distributions of the parent molecules and different daughter molecules (like OH or [OI]) within 10 km to the nucleus center. This means that a DSMC model has to be developed to simulate this highly anisotropic gas outflow which can be in turn adopted for computing the motion and density distribution of the photo-fragments. In this work, we will present the results from a preliminary study using the OH radicals and oxygen atoms generated in photodissociation of water molecules as tracers to examine the basic ingredients of the inner coma of comet 67P.

The DSMC method was proposed by Bird (1994) which can be applied to all regimes of gas flow. It can solve the Boltzmann equation by using direct simulation of a large amount of particles and collisions. In the DSMC method, we divide the simulation space into a lot of cells assuming each particle only can collide with other particles in the same cells in one time step (Crifo et al. 2004; Combi et al. 2004). The cell size must be smaller than the local mean free path of the molecules. A parallel 3D DSMC code named PDSC^{++} using an unstructured grid has been developed by Wu et al. (2004) and Su et al. (2010, 2013). It has been parallelized for cluster calculations by high-speed computers and adopted for the numerical simulation of the rarified gas flow near the cometary nucleus (Finklenburg et al. 2014). To run the DSMC simulation on the cluster with 96 CPUs at Taiwan's National

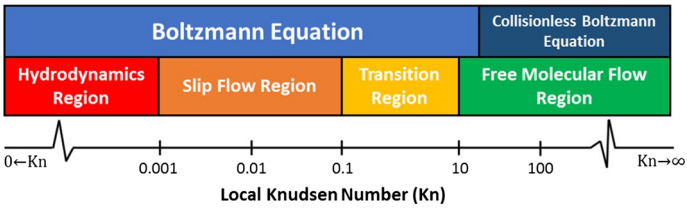

Fig. 1 Classification of the flow regimes from the fully hydrodynamic region to the free molecular flow region

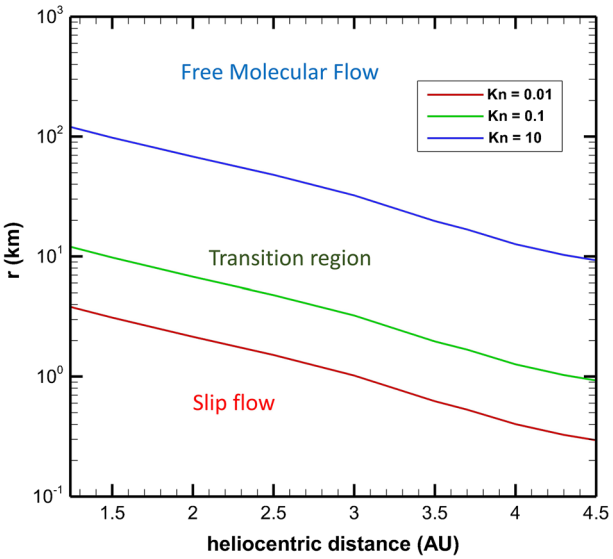

Fig. 2 An illustration of the approximate size of the collisional zone of the expanding gas flow from comet 67P at different heliocentric distances

High-Performance Computing Center, we use a grid with one million cells and 10 million simulation particles.

The model calculation presented here is specific to the initial phase of the Rosetta mission when comet 67P was at a heliocentric distance of about 3 AU and that the Hapi region was sunlit. This situation is probably most extreme in terms of the topological effect on the expanding gas flow. The heterogeneity of the surface materials and geomorphological structure of the nucleus surface leads to strong changes in the ice sublimation process at different spatial and temporal scales. This can be testified by the highly variable gas production rate over one rotational period as reported by Haessig et al. (2015).

The shape model produced by the OSIRIS science camera team (Sierks et al. 2015) is used to determine the sunlit condition. The surface of the comet nucleus is covered by many facets (see Fig. 3). To simplify the calculation, we have neglected the thermal conduction effect of the nucleus subsurface material by prescribing a surface distribution of sublimation rate. Two models are considered here. The first one assumes that the gas only emits from the Hapi region. The distribution of the source strength is based on the probability analysis of the source strength of dust jet features for a certain sunlit condition as described in Lin et al. (2015). The total gas production rate of 3×10^{25} H_2O s^{-1} specific to the Hapi source zone was taken from the estimate of $10^{25} \sim 4 \times 10^{25}$ H_2O s^{-1} given by Gulkis et al. (2015). This highly simplified case allows us to determine whether the back flow from the day side to the night side as found by Combi (1996) can take place in the present case or not.

The second model describes a more realistic case. That is, besides the sunlit Hapi region, other areas could emit gas with or without solar illumination. This is done by ascribing a minimum outgassing rate of 10 % of the peak value given in Fig. 3.

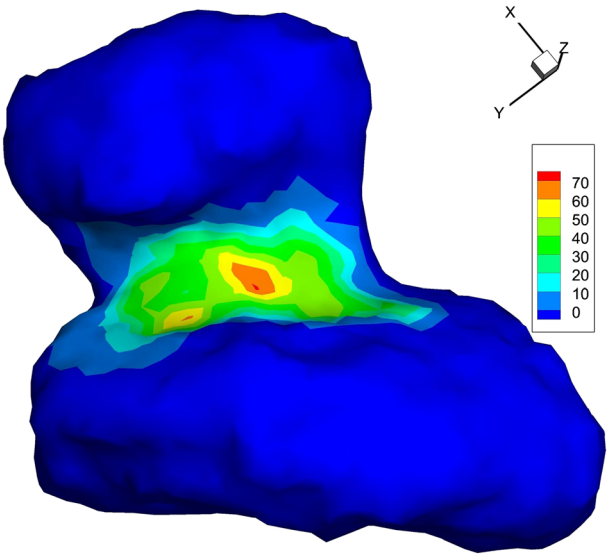

Fig. 3 An illustration of the shape model of comet 67P covered with the spatial distribution of the source regions in the neck region. The *color scale* is from 0 to 100 (from Lin et al. 2015)

3 Results

We consider the photochemical reactions: $H_2O + hv \rightarrow H + OH$ and $H_2O + hv \rightarrow O + H_2$, respectively. The photodissociation rate of water molecules leading to the formation of OH radicals is 1.03×10^{-5} s^{-1} at a heliocentric distance of 1 AU while the secondary channel for the O (^{1}D) production has a corresponding dissociation rate of 1.35×10^{-6} s^{-1} (Schmidt et al. 1988). [In subsequent discussion in this work, OI and O(^{1}D) are interchangeable.]

Our numerical procedure is as follows. A DSMC calculation is first performed with pure water molecules. The initial velocity distribution at the nucleus surface is approximated to be a half-Maxwellian distribution with a thermal temperature of 160 K. In the first case, we have chosen to model the situation when the neck region is at maximum solar illumination. Because of the small number of the OH radicals or the oxygen atoms created by photodissociation within a few km to the comet in each run, it is convenient to model their production and subsequent dynamics by adopting a test particle approach. That is, test particles representing new photo-fragments are introduced into different cells of the simulation box each tagged with weighting factors proportional to the corresponding photodissociation rates of water molecules at those positions. The initial velocities (Δv) of the new oxygen atom and H_2 molecules in the moving frame of the H_2O parent molecule are determined by the consideration of momentum conservation. With an excess energy of 3.5 eV (Schmidt et al. 1988), the excess speed of the oxygen atom can be estimated to be $\Delta v = 2.1$ km s^{-1}. By the same token, $\Delta v = 1.46$ km s^{-1} for the OH radicals. With an isotropic emission direction, the velocity of the oxygen atom so created will be given by $\vec{v}' = \vec{v} + \Delta\vec{v}$ where $\vec{v}$ is the flow velocity of the parent water molecule obtained from the DSMC calculation. The subsequent motion of the oxygen atom is followed in the following manner. First, in each time step the collisional mean-free-path λ is computed by defining

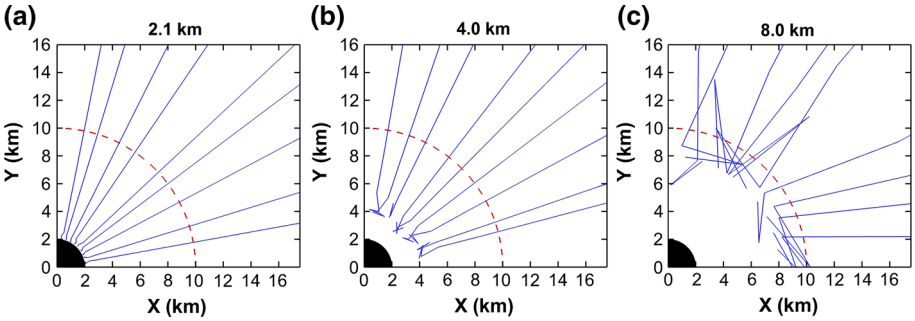

Fig. 4 Trajectories of the photo-fragments created in different spherically symmetric source regions surrounding a nucleus with a gas production rate of 3×10^{25} molecules s^{-1}; **a** collisional zone; **b** quasi-collisional zone; and **c** nearly-collisionless zone. The *dashed circle* shows the dimension of the DSMC simulation box

$$\lambda = \frac{v_{th}}{v_r \sigma n}$$

where v_{th} is the mean thermal speed of H_2O molecules, v_r is the relative velocity, σ is the collisional cross section, and n is the local H_2O number density. The impact probability (P) of a particle traveling for a distance L is then given by

$$P = \left(1 - e^{-\int \frac{ds}{\lambda}}\right).$$

It can be seen that P increases along the flight path of the oxygen atom before the next collision. At which point a collision between the oxygen atom and a water molecule will take place of not is determined by calling a random number (ε) between 0 and 1: if $\varepsilon < P$, a collision will take place. Otherwise, the oxygen atom will move forward by a distance of $\Delta s = v\Delta t$ and a new random number will be called to check if a collision would happen or not. If a collision between the oxygen atom and a water molecule happens, a hard sphere scattering model will be applied to compute the new velocity of the oxygen atom. It is in this way that the oxygen atom will gradually share its excess energy with the background gas and be assimilated into the expanding coma if collisions are frequent enough. Figure 4 shows examples of the trajectories of oxygen atoms created at different radial distances from the nucleus center. For source region inside the collisional zone, the oxygen atoms will quickly become co-moving with the water molecules in nearly-radial direction (see Fig. 4a). But for source regions outside the collisional zone, only a small fraction of the oxygen atoms will be assimilated while the rest will continue with their motion in different directions (see Fig. 4b, c). That the particle trajectories appear to point outward in Fig. 4c is because of the fact that the new atoms would usually bounce back if they move towards the dense coma region.

3.1 Case I with Only the Hapi Source Region

Figure 5 summarizes the flow fields of different species of the water-group neutrals on a cross section (on the XZ-plane) containing the long axis of the comet 67P and the YZ-plane in the orthogonal direction. The non-spherical expansion close to the nucleus is because of the concave contour of the Hapi region being sandwiched between the cliff-like Seth and Hathor regions.

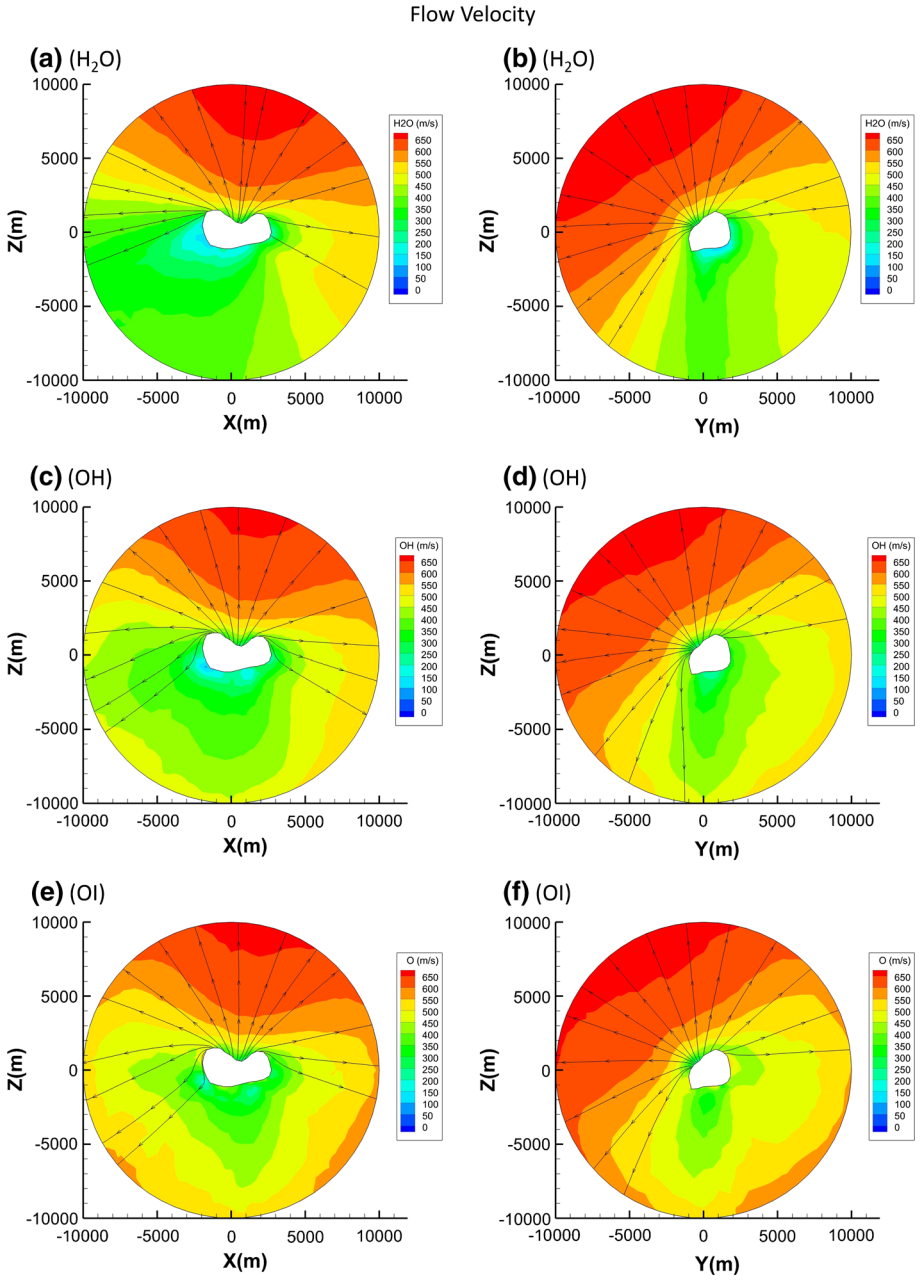

Fig. 5 DSMC results of the flow fields of the H_2O molecules (**a**, **b**) and the photo-fragments: OH (**c**, **d**) and O-atoms (**e**, **f**) from the test particle calculation. The *left panels* (2D representation on the XZ plane) and *right panels* (2D representations on the YZ plane) are shown to compare the differences in different viewing conditions

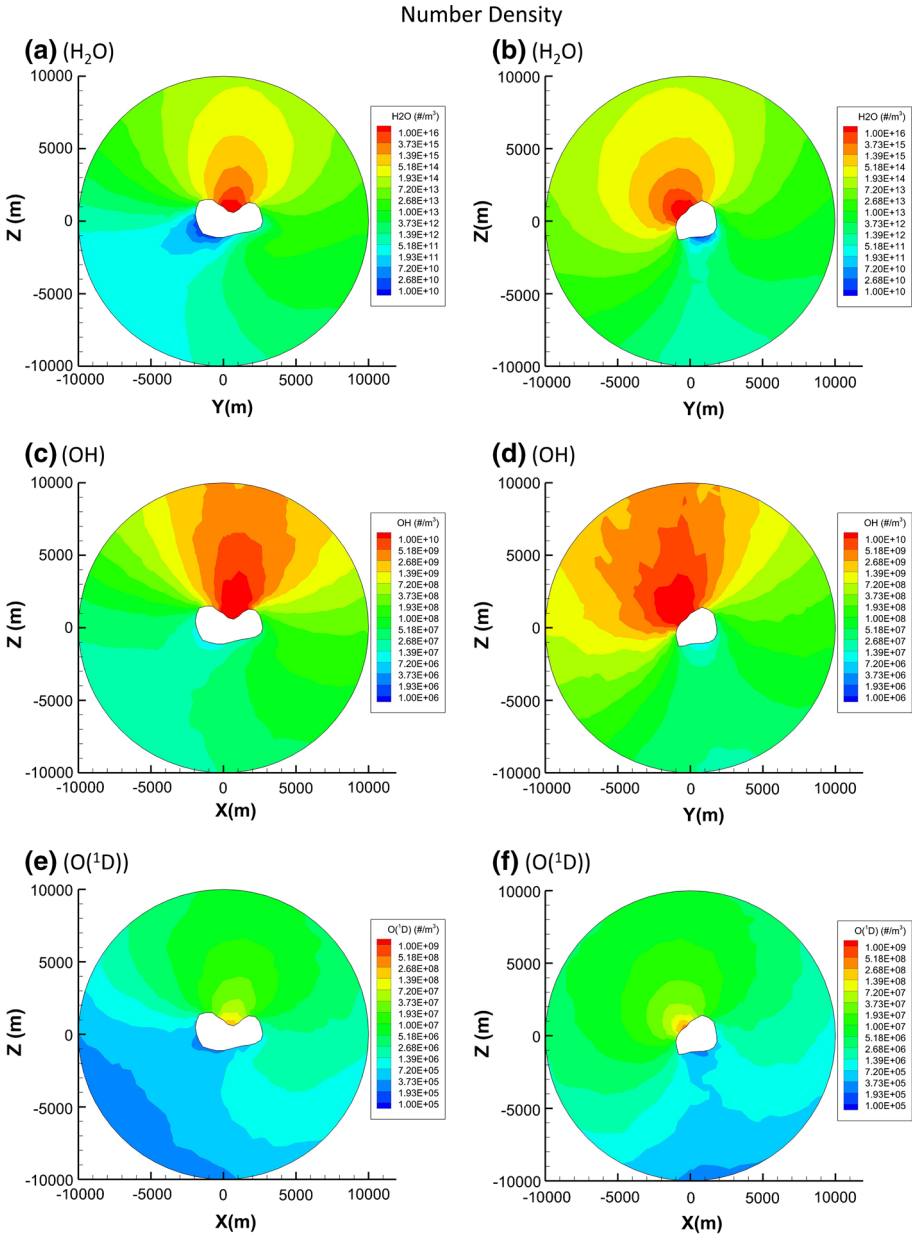

Fig. 6 DSMC simulation of the H_2O number density distributions (**a**, **b**) and test particle results of the OH radicals (**c**, **d**) and oxygen atoms (**e**, **f**) of comet 67P at 3 AU. Projection and viewing condition the same as described in Fig. 5

In spite of the lack of gas emission from the night side, there is no H_2O stream lines connecting the sunlit side to the non-sunlit side (Fig. 5a, b). In the test particle calculation, the flow fields of the OH and O-atoms follow closely that of the water molecules near the

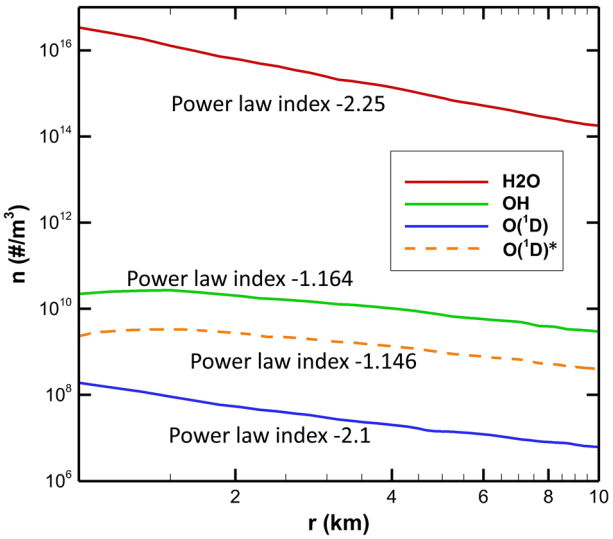

Fig. 7 The radial dependence of the number density of the water molecules along the sunlit direction, OH radicals and OI atoms, respectively. The *dashed line* shows the result without collisional quench

Hapi region. We do find some differences in the vicinity of the terminator in some cases (Fig. 5c–f).

Figure 6 shows the number distributions of the water molecules, OH radicals and oxygen atoms within 10 km to the comet center. It is the nature of our hybrid approach with finite number of test particles in the numerical calculation that the spatial distributions of OH and OI appear to be rugged in comparison to the smooth profile of the water molecules.

To examine the numerical results further, we plot in Fig. 7 the number density distributions of these three types of gas molecules along the Sun-comet line in Fig. 6a, c, e. It can be seen that the radial dependence of n(H_2O) follows a power law ($n\alpha r^{-k}$) with an index of $k = 2.25$ which fits the picture of non-spherical expansion well. As for n(OH), $k \sim 1.1$ for $r > 2$ km which is just the consequence of continuous injection of new particles by water photodissociation.

If we only consider the number distribution of neutral oxygen atoms, a similar curve will result. However, the excited state of O(^{1}D) is subject to collisional quench with a quenching cross section of 1.8×10^{-16} cm^2 (Bisikalo et al. 2015; Tenishev et al. 2011) in the innermost region of the coma before the radiative decay time of 130 s. Figure 7 compares the O(^{1}D) number density distribution for the cases with and without taking into account the collision effect. The O(^{1}D) number density and hence the red line emission should be suppressed significantly within a few km to the nucleus in the actual situation. The radial slope of the O(^{1}D) number density distribution beyond the collisional zone follows a trend of $n \sim r^{-k}$ with $k \sim 2$.

Figure 8 shows the column number densities (N) of OH and OI, respectively. It is noted that N(OH) $\gg$ N(O(^{1}D)) because the branching ratio of $H_2O + hv \rightarrow H + OH$ is a factor of 25 larger than that of $H_2O + hv \rightarrow H_2 + O(^1D)$. Furthermore, O(^{1}D) is subject to collisional quenching close to the nucleus as discussed before.

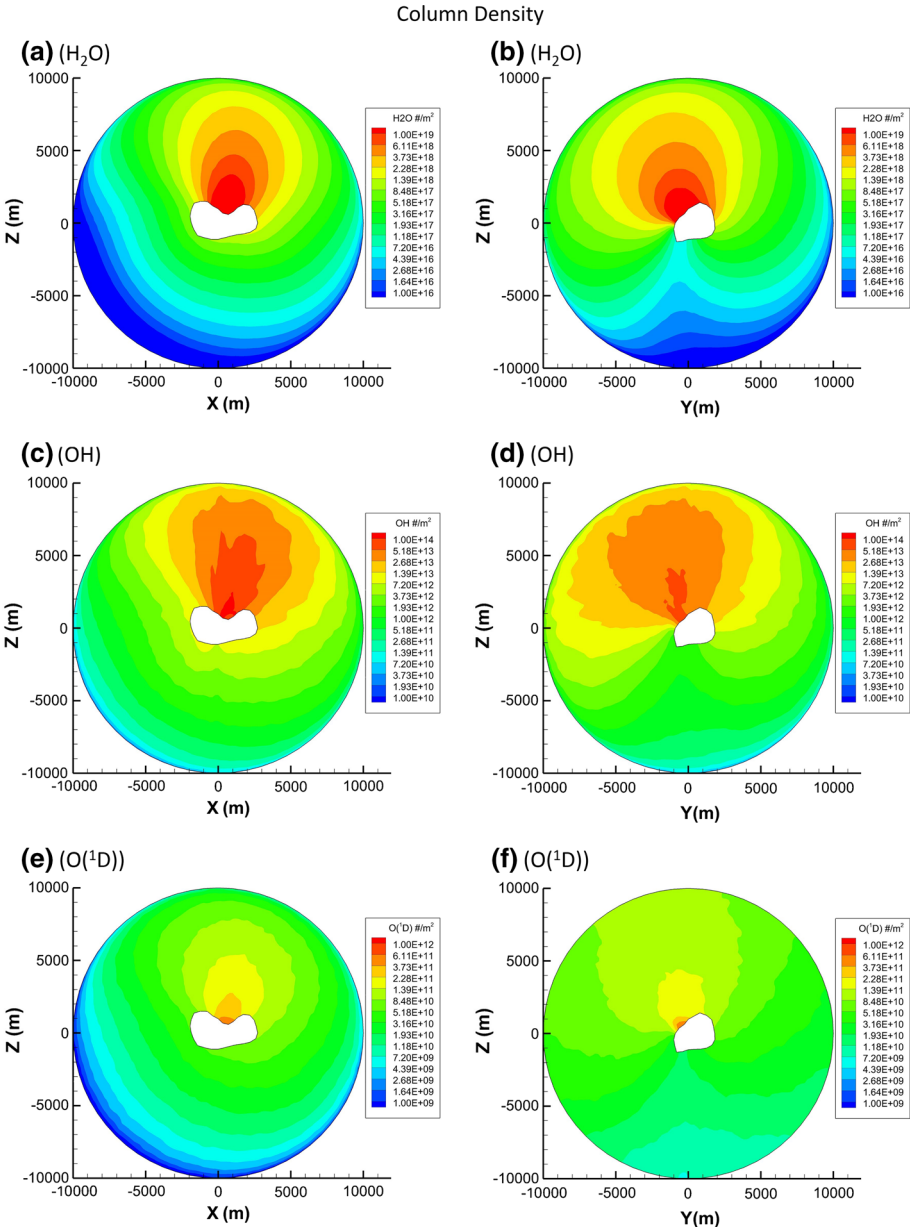

Fig. 8 The column number densities of water molecules from DSMC simulation (**a**, **b**) and test particle results of the OH radicals (**c**, **d**) and oxygen atoms (**e**, **f**) of comet 67P at 3 AU. Projection and viewing condition the same as described in Fig. 5

Because of the super-divergence of the gas flow from the neck region, the column density (or optical brightness) integrated along the line-of-sight perpendicular to the direction of the rotation axis is dominated by the portion close to the nucleus within the simulation box. Hat mapping of the brightness distributions of OH and [OI] can give us

information on the short-term, almost instantaneous outgassing condition even the background emission produced by more extended coma would certainly contribute. Another point is that, in the test particle runs, the photodissociation of OH and photoionization of the oxygen atoms can be easily included. Because the relevant time scales are all much larger than the dynamical time scale of the gas flow within the region of interest ($\sim$20 s), their density profiles are basically determined by the respective source rates.

3.2 Case II with the Hapi Source Region and Background Outgassing

During the first part of the Rosetta mission the ROSINA instrument detected peak H_2O flux near the illuminated Hapi region but it subsided when Imhotep was in view at which time CO and CO_2 instead became the dominant species (Haessig et al. 2015). Also, even though the southern hemisphere was in darkness, outgassing activity from the unilluminated areas with relatively large abundances of CO and CO_2 ($CO_2/H_2O \sim 60$ %) was observed by the VIRTIS experiment (Bockelee-Morvan et al. 2004). The presence of this background outflow will probably act to reduce the trend of super-expansion. To explore the situation of non-zero gas sublimaton from the other areas external to Hapi, we have performed DSMC calculation with water outgassing rate set to be 10 % of the peak value shown in Fig. 3. (The initial thermal temperature of the "background" gas flow is assumed to be 160 K in this test case even though it should be smaller in the dark side.)

Figure 9 shows the flow pattern, number density and column density of the water molecules. The existence of small amount of gas emission is effective in reducing the degree of super-expansion of the gas outflow from the Hapi region. The number density distribution and column density distribution are anisotropic because of the enhanced emission from the neck.

The same distributions of OH are shown in Fig. 10. What is interesting is that its flow pattern is quite similar to that of H_2O while the number density distribution and column number density distribution are both isotropic. One reason is probably because while the Hapi region on the northern side is a hot spot the southern hemisphere has a bigger cross sectional area then the ends of the two lobes. In reality, the number density of OH should be much diminished in the south because the winter hemisphere emitted little water molecules. Furthermore, in the assumed solar illumination condition of the present simulation, a part of the coma in the south will be in shadow and shielded from solar radiation. This means we should expect a strong outflow of OH from the sunlit Hapi region but much less from the opposite side.

Because of their larger excess velocity at production, the $O(^1D)$ atoms could gain a larger outflow speed in comparison with OH (i.e., 650 vs. 600 m s^{-1}) as shown in Fig. 11. Their number density distribution and column density distribution match those of the water molecules very well. This is because the strong quenching collision effect in the innermost coma tends to restrict their presence to the location where they are created. On the other hand, the additional consideration of the shadow effect will reduce the $O(^1D)$ brightness above the southern hemisphere.

4 Summary and Discussion

The possibility of including daughter molecules like OH and OI from photodissociation in the inner coma of comet 67P at the weak coma phase when the heliocentric distance was about 3 AU is considered. It is shown that we can treat the photo-fragments (i.e., OH

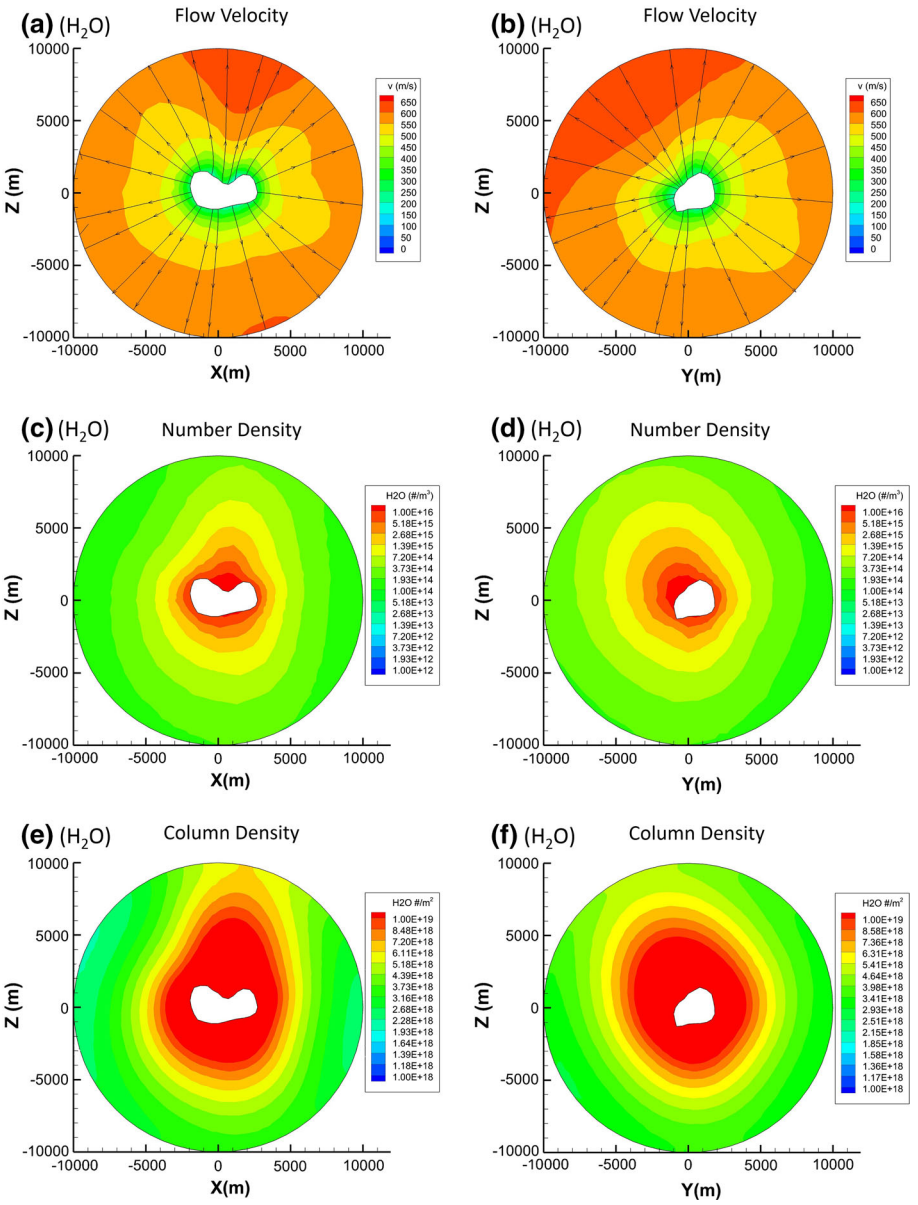

Fig. 9 DSMC coma simulation results for H_2O with (10 %) background outgassing in addition to the Hapi source region: *Upper panels*: the flow fields and streamlines; **b** *Middle panels*: the water number density distributions; and **c** column number density distributions

hydroxyl radicals and oxygen atoms) as test particles with a hybrid approach. This scheme is partly necessitated by the small number of new fragments in comparison to the background coma composed of water (and CO_2, CO and O_2) molecules. Within a few collisional radii, their motion would be affected by intra-particle collisions with the parent molecules.

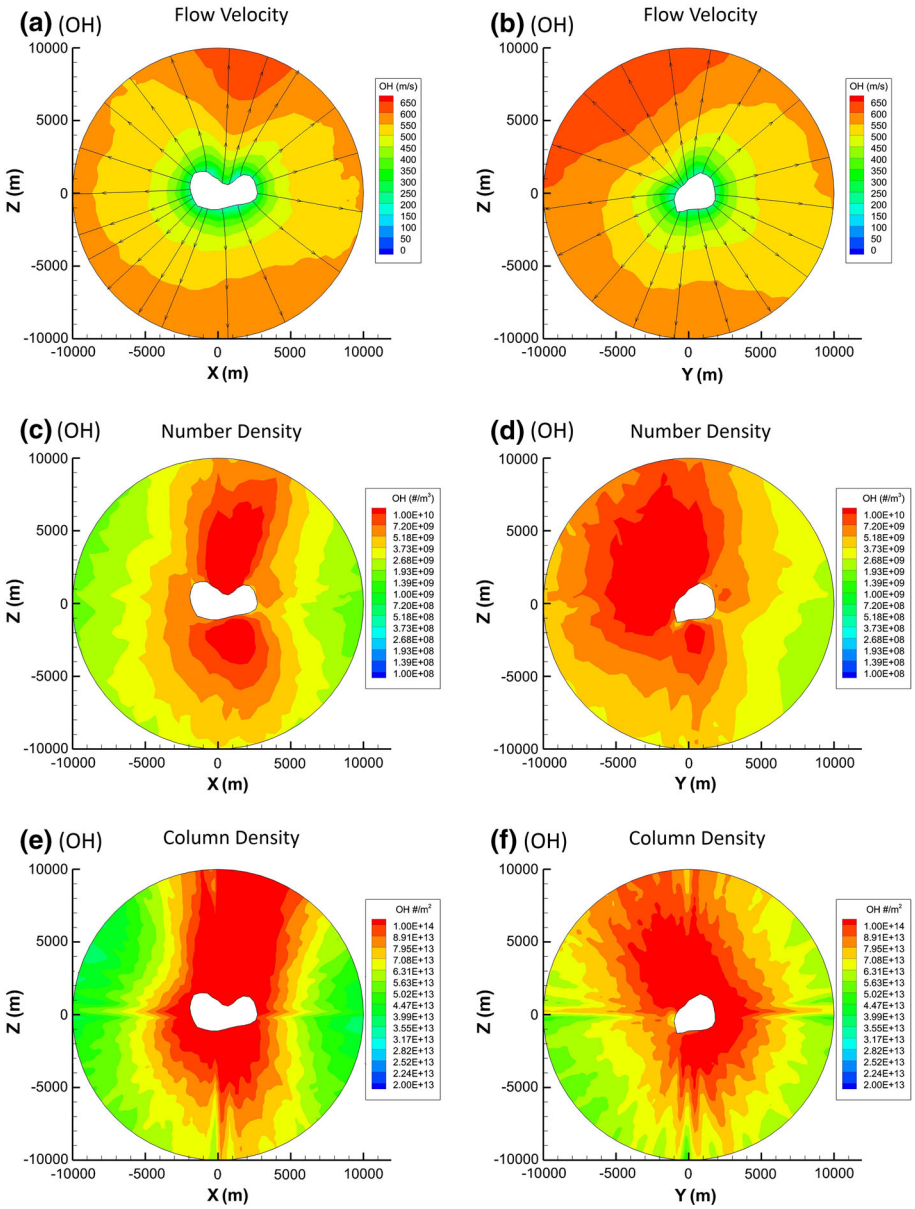

Fig. 10 Same as Fig. 9 for OH

There are a number of differences between the previous treatment by Combi (1996) and the present work. The first one is that a more realistic shape model is used here. The second one has to do with the fact that the outgassing rate considered here is much less the values used in the study of Combi (1996). This is probably one reason why no day-to-night backflow occurs in our simulations. The very small size of the collisional zone means that all water molecules would be able to escape without bing partially recycled to the night

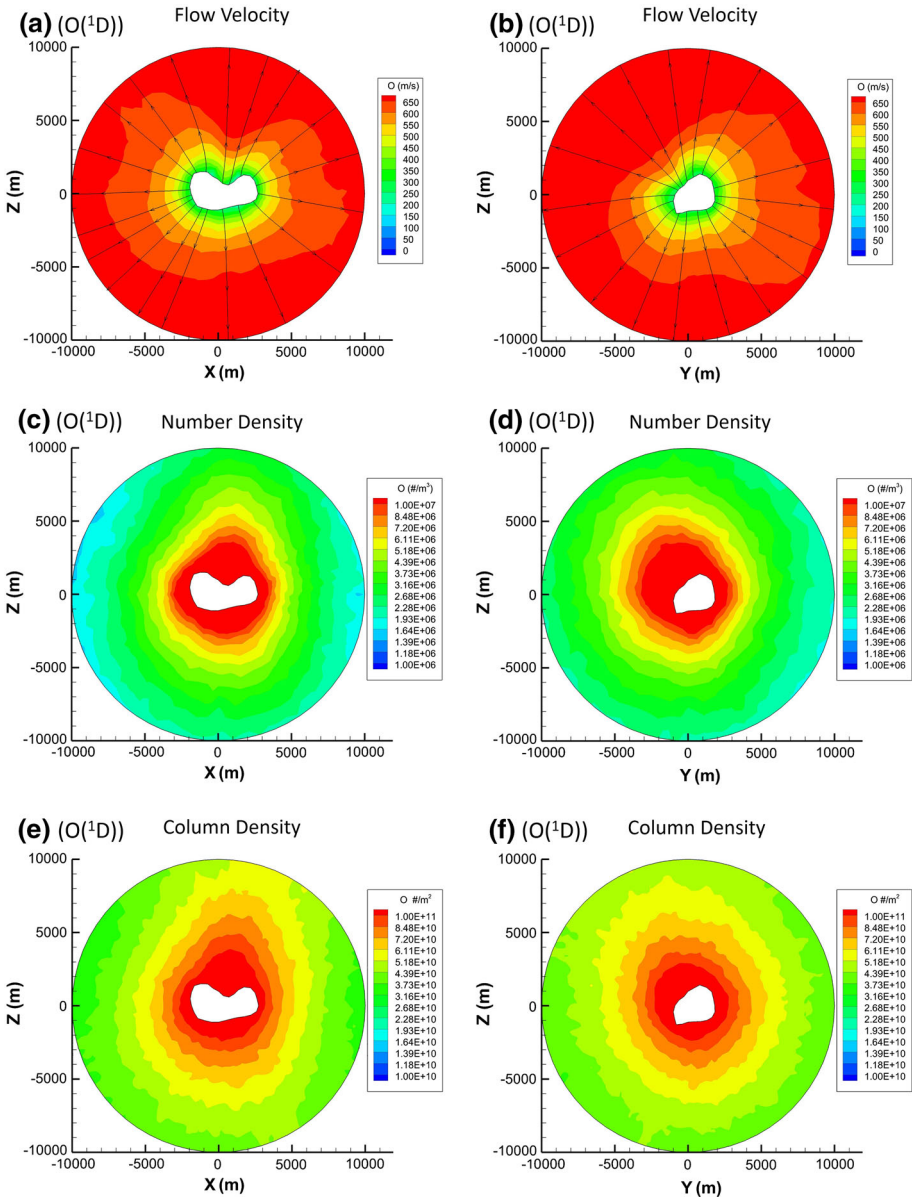

Fig. 11 Same as Fig. 9 for O(^{1}D)

side. This is so even when there is no gas emission from the nightside as demonstrated in Case I with only the Hapi source region.

The most recent report from the ALICE experiment (Feldman et al. 2015) showed that photoelectrons are very effective in dissociating H_2O, CO and CO_2 into the radical and atomic fragments (OH, O, C and H). The presence of other fast dissociative process in addition to photodissociation in the near-nucleus region of comet 67P is further supported by the gas coma observations of the OSIRIS scientific camera which reported strong

optical emissions from OH and O(^{1}D) not accounted for by photolytic effect (Bodewits et al. 2016). For photoelectron impact dissociation, several species other than H_2O, namely, CO_2, CO and O_2 could all be important. In future work, we will apply the present DSMC/hybrid model to the coma dynamics and spatial distribution of OH and O(^{1}D) at different time periods as the comet moved around perihelion by including both photodissociation and photoelectron impact effects.

Acknowledgments We thank the reviwers for useful comments and suggestions in improving the content of this paper. We are also indebted to Dr. Zhong-Yi Lin, Dr. Dennis Bodewits, Jui-Chi Lee, and the Rosetta OSIRIS science team for helpful discussions. This work was supported by MOST 104-2119-M-008-024 (TANGO II) and MOST 104-2111-M-008-020 (Space) in Taiwan and MSTDF Grant No. 017/2014/A1 and 039/2013/A2 in Macau.

References

A. Bhardwaj, S. Raghuran, A coupled chemistry-emission model for atomic oxygen green and red-doublet emissions in the comet C/1996 B2 Hyakutake. Astrophys. J. **748**(1), 18 (2012)

A. Bieler, K. Altwegg, H. Balsiger et al., Abundant molecular oxygen in the coma of comet 67P/Churyumov–Gerasimenko. Nature **526**, 678 (2005)

G.A. Bird, *Molecular Gas Dynamics and the Direct Simulation of Gas Flows* (Clarendon Press, Oxford, 1994)

D.V. Bisikalo, V.I. Shematovich, J.-C. Gérard et al., Monte Carlo simulation of metastable oxygen photochemistry in cometary atmospheres. Astrophys. J. **798**, 21 (2015). doi:10.1088/0004-637X.798/1/21

N. Biver, D. Bockelee-Morvan, P. Colom et al., Evolution of the outgassing of comet Hale-Bopp (C/1995 OI) from radio observations. Science **275**, 1915 (1997)

D. Bockelee-Morvan, J. Crovisier, E. Gerard, Retrieving the coma gas expansion velocity in P/Halley, Wilson (1987 VII) and several other comets from the 18-cm OH line shapes. A&A **238**, 382 (1990)

D. Bockelee-Morvan, J. Crovisier, M.J. Mumma, H.A. Weaver, in *The composition of cometary volatiles, in comets II*, ed. by M.C. Festou, H.U. Keller, H.A. Weaver (LPI, Arizona, 2004), pp. 391–423

D. Bodewits, L. M. Lara, M. F. A'Hearn, et al. Orbital evolution of the physical environment in the inner coma of 67P/Churyumov–Gerasimenko. A&A (2016)

A.L. Cochran, Atomic oxygen in the comae of comets. Icarus **198**, 181 (2008)

A.L. Cochran, W.D. Cochran, Observations of O(1S) and O(1D) in spectra of C/1999 S4 (LINEAR). Icarus **154**, 381 (2001)

M.R. Combi, Time-dependent gas kinetics in tenuous planetary atmospheres: the cometary coma. Icarus **123**, 207–226 (1996)

M.R. Combi, W.M. Harris, W.H. Smyth, in *Gas Dynamics and Kinetics in the Cometary Coma: Theory and Observations, in Comets II*, ed. by M.C. Festou, H.U. Keller, H.A. Weaver (LPI, Arizona, 2004), pp. 523–552

J.F. Crifo, M. Fulle, N.I. Koemle, K. Szego, in *Nuclues-Coma Structural Relationships: Lessons From Physical Models, in Comets II*, ed. by M.C. Festou, H.U. Keller, H.A. Weaver (LPI, Arizona, 2004), pp. 471–503

J. Crovisier, The photodissociation of water in cometary atmospheres. Astron. Astrophys. **213**, 459–464 (1989)

P.D. Feldman, A.L. Cochran, M.R. Combi, in *Spectroscopic Investigations of Fragment Species in the Coma, in Comets II*, ed. by M.C. Festou, H.U. Keller, H.A. Weaver (LPI, Arizona, 2004), pp. 425–447

P.D. Feldman, M.F. A'Hearn, J. Bertaux et al., Measurements of the near-nucleus coma of comet 67P/Churyumov–Gerasimenko with the Alice far-ultraviolet spectrograph on Rosetta. A&A (2015). doi:10.1051/0004-6361/201525925

M.C. Festou, The density distribution of neutral compounds in cometary atmospheres 1. Model and equations. Astron. Astrophys. **95**, 69 (1981)

U. Fink, J.R. Johnson, Luminosity and spatial distribution of the [OI] 6300 A emission in comets. Astron. J. **89**, 1565 (1984)

S. Finklenburg, N. Thomas, C.-C. Su et al., The spatial distribution of water in the inner coma of Comet 9P/Tempel 1: comparison between models and observations. Icarus **236**, 9–23 (2014)

S. Gulkis, M. Allen, P. von Allmen et al., Surface properties and early activity of comet 67P/Churyumov–Gerasimenko. Science **347**, aaa0709 (2015)
M. Haessig, K. Altwegg, H. Balsiger et al., Time variability and heterogeneity in the coma of 67P/Churyumov–Gerasimenko. Science **347**, aaa0276 (2015)
L. Haser, Distribution d'intensite dans la tete d'une comete. Bull. Acad. R de Belgique Classe de Sci. **43**(5), 740–750 (1957)
W.-H. Ip, On photochemical heating of cometary comae: the cases of H_2O and CO-rich comets. Astrophys. J. **264**, 726 (1983)
W.-H. Ip, An overview of gas phenomena in Comet Halley. Adv. Space Res. **5**, 233 (1985)
Y. Liao, C. C. Su, R. Marschall, et al., 3D Direct Simulation Monte Carlo modelling of the inner gas coma of comet 67P/Churyumov–Gerasimenko: a parameter study. Earth Moon Planets (2016) (in press)
Z.-Y. Lin, W.-H. Ip, I.-L. Lai et al., Morphology and dynamics of jets of comet 67P/Churyumov–Gerasimenko: early phase development. A&A (2015). doi:10.1051/0004-6361/201525961
S. Raghuram, A. Bhardwaj, M. Galand, Prediction of forbidden ultraviolet and visible emissions in comet 67P/Churyumov-Gerasimenko. Accepted in Earth and Planetary Astrophysics (2016) arXiv:1511.05496
L. Roy, K. Altwegg, H. Balsigeret et al., Inventory of the volatiles on comet 67P/Churyumov–Gerasimenko from Rosetta/ROSINA. A&A **583**, A1 (2015). doi:10.1051/0004-6361/201526450
M. Rubin, V.M. Tenishev, M.R. Combi et al., Monte Carlo modeling of neutral gas and dust in the coma of comet 1/P Halley. Icar **213**, 655 (2011)
D.G. Schleicher, M.F. A'Hearn, The fluorescence of cometary OH. Astrophys. J. **331**, 1058 (1988)
H.U. Schmidt, R. Wegmann, W.F. Huebner, D.C. Boice, Cometary gas and plasma flow with detailed chemistry. Comput. Phys. Commun. **49**(1), 17–59 (1988)
H. Sierks, C. Barbieri, PhL Lamy et al., On the nucleus structure and activity of comet 67P/Churyumov–Gerasimenko. Science **347**, aaa1004 (2015)
C. Snodgrass, C. Tubiana, D.M. Bramich, K. Meech, H. Boehnhardt, L. Barrera, Beginning of activity in 67P/Churyumov–Gerasimenko and predictions for 2014–2015. A&A **557**(1), A33 (2013)
C.-C. Su, K.-C. Tseng, H.M. Cave, J.-S. Wu, Implementation of a transient adaptive sub-cell module for the parallel DSMC code using unstructured grids. Comput. Fluids **39**, 1136–1145 (2010)
C.-C. Su, Parallel Direct Simulation Monte Carlo (DSMC) methods for modeling rarefied gas dynamics. Ph.D. thesis, National Chiao Tung University, Taiwan (2013)
V. Tenishev, M.R. Combi, M. Rubin, Numerical simulation of dut in a cometary coma: application to comet 67P/Churyumov–Gerasimenko. ApJ **732**, 104 (2011)
W.-L. Tseng, D. Bockelee-Morvan, J. Crovisier, P. Colom, W.-H. Ip, Cometary water expansion velocity from OH line shapes. A&A **467**, 729 (2007)
J.-S. Wu, K.-C. Tseng, F.-Y. Wu, Parallel three-dimensional DSMC method using mesh refinement and variable time-step scheme. Comput. Phys. Commun. **162**, 166 (2004)
X. Xie, M.J. Mumma, Monte Carlo simulation of cometary atmospheres: application to comet P/Halley at the time of the Giotto spacecraft encounter I. Isotropic model. Astrophys. J. **464**, 442 (1996a)
X. Xie, M.J. Mumma, Monte Carlo simulation of cometary atmospheres: application to comet P/Halley at the time of the Giotto spacecraft encounter II. Axisymmetric model. Astrophys. J. **464**, 457 (1996b)
V.V. Zakharov, A.V. Rodionov, G.A. Lukianov, J.F. Crifo, Monte-Carlo and multifluid modelling of the circumnuclear dust coma II. Aspherical-homogeneous, and spherical-inhomogeneous nuclei. Icarus 201, **358** (2009)